

Elevator, Escalator or Neither? Classifying Pedestrian Conveyor State Using Inertial Navigation System

TIANLANG HE, ZHIQIU XIA, and S.-H. GARY CHAN, The Hong Kong University of Science and Technology, Hong Kong S.A.R.

Knowing a pedestrian's *conveyor state* of "elevator," "escalator," or "neither" is fundamental in many applications such as indoor navigation and people flow management. We study, for the first time, classifying the conveyor state of a pedestrian, given the multimodal INS (inertial navigation system) readings of accelerometer, gyroscope and magnetometer sampled from the pedestrian phone. This problem is challenging because the INS signals of the conveyor state are entangled with unpredictable independent pedestrian motions, confusing the classification process. We propose ELESON, a novel, effective and lightweight INS-based deep learning approach to classify whether a pedestrian is in an **elevator**, **escalator** or **neither**. ELESON utilizes a causal feature extractor to disentangle the conveyor state from pedestrian motion, and a magnetic feature extractor to capture the unique magnetic characteristics of moving elevators and escalators. Given the results of the extractors, it then employs an evidential state classifier to estimate the confidence of the conveyor states. Based on extensive experiments conducted on real pedestrian data, we demonstrate that ELESON outperforms significantly previous INS-based classification approaches, achieving 14% improvement in F1 score, strong confidence discriminability of 0.81 in AUROC (Area Under the Receiver Operating Characteristics), and low computational and memory requirements for smartphone deployment.

CCS Concepts: • **Human-centered computing** → **Ubiquitous and mobile computing systems and tools**.

Additional Key Words and Phrases: Conveyor state classification, inertial navigation system, causal representation learning, confidence estimation

ACM Reference Format:

Tianlang He, Zhiqiu Xia, and S.-H. Gary Chan. 2018. Elevator, Escalator or Neither? Classifying Pedestrian Conveyor State Using Inertial Navigation System. In . ACM, New York, NY, USA, 19 pages. <https://doi.org/XXXXXXXX.XXXXXXX>

1 INTRODUCTION

Knowing whether a phone user is taking an elevator, escalator, or neither is vitally important for indoor navigation systems, enabling timely updates of the user's floor transition. Yet another application is to analyze pedestrian flow and conveyor preference in a venue, shedding insights on user behavior, flow management and conveyor capacity planning [1–6]. For the first time, we study classifying a pedestrian in one of the three *conveyor states* of "elevator," "escalator" and "neither," given the INS (inertial navigation system) readings from accelerator (i.e. acceleration), gyroscope (i.e. angular velocity) and magnetometer (i.e. geomagnetic, or simply magnetic field) sampled from the pedestrian phone. Compared with other sensors, such as barometer, INS is better suited for this task due to its real-time performance and widespread availability on smartphones.

The conveyor state classification problem is challenging because the measured INS signals are a superposition from both conveyor state and pedestrian motions, i.e., the features of conveyor state are disrupted and entangled with those due to unpredictable, arbitrary and diverse motions carried out by the pedestrian in the state. Most of

Permission to make digital or hard copies of all or part of this work for personal or classroom use is granted without fee provided that copies are not made or distributed for profit or commercial advantage and that copies bear this notice and the full citation on the first page. Copyrights for components of this work owned by others than ACM must be honored. Abstracting with credit is permitted. To copy otherwise, or republish, to post on servers or to redistribute to lists, requires prior specific permission and/or a fee. Request permissions from permissions@acm.org.

Proc. ACM Interact. Mob. Wearable Ubiquitous Technol., June 03–05, 2018, Woodstock, NY

© 2018 Association for Computing Machinery.

ACM ISBN 978-1-4503-XXXX-X/18/06...\$15.00

<https://doi.org/XXXXXXXX.XXXXXXX>

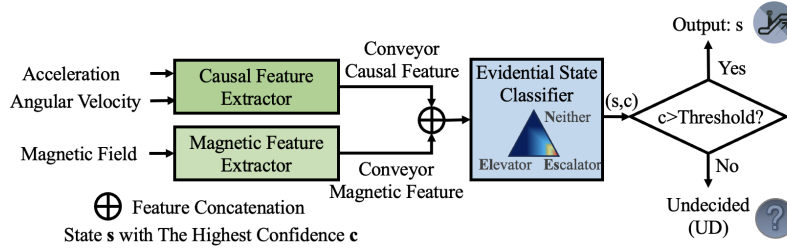


Fig. 1. System overview of ELESON.

these pedestrian motions, such as fidgeting, swinging and browsing, are largely independent of the state, therefore appearing as "noise" to the state signals. Though INS signals have been extensively studied for classification tasks (e.g., gesture recognition, gait detection, human action recognition, fall detection, etc. [7–10]), these studies treat, train and infer the INS signals as a whole without disentangling the conveyor signals from user motions. This leads to noisy and unreliable classification results, greatly limiting the accuracy (as demonstrated in our experiments).

To tackle the problem, we need to address the following three critical questions: 1) Given the plethora of possible pedestrian motions, it is unrealistic to exhaustively conceive and label them in training. Without the need for any pedestrian motion labeling, how can we extract the features of conveyor states from their entanglement with pedestrian motion using motion signals, i.e., acceleration and angular velocity? 2) How can we leverage magnetometer to appropriately differentiate the temporal magnetic features between moving elevator and escalator, so as to further boost the classification effectiveness? 3) How can we support sound decision by providing a confidence of each conveyor state that properly reflects the similarity of target INS signals with the training data?

We propose ELESON, a novel lightweight INS-based deep learning approach to classify a pedestrian being in **e**levator, **e**scalator, or **n**either based on multimodal data. We show in Figure 1 the classification process of ELESON, which consists of the following three major steps:

- (1) *Causal feature extractor to segregate conveyor state from arbitrary pedestrian motion:* We propose a causal feature extractor which derives from the motion signals (acceleration and angular velocity) the causal features of elevator and escalator through a causal decomposition, in such a way that the extracted features are independent of pedestrian motions. To achieve that, we present a novel intervention simulation loss function in the training process.
- (2) *Magnetic feature extractor to differentiate the magnetic pattern between moving elevator and escalator:* Observing the differences in magnetic pattern between transporting enclosed elevator and open escalator, we propose a magnetic feature extractor to capture properly the features in order to boost the classification accuracy. We further introduce an adversarial learning approach in the extractor to make the classification more robust against pedestrian motion.
- (3) *Evidential state classifier to estimate state confidence:* After the feature extractors, we propose, based on evidence theory, an evidential state classifier to estimate the confidence (between 0 and 1) for each conveyor state. Our confidence reflects the signal similarity with that of the training data. Given the confidence, the pedestrian is classified to the state with the highest confidence provided such confidence is above a certain threshold, or "undecided" (UD) otherwise.

We have collected substantial amount of annotated real data, where pedestrians take different elevators and escalators with arbitrary random motions. We compare ELESON with state-of-the-art classification approaches

that treat INS signals as a whole. ELESON is shown to outperform significantly, achieving 14% improvement in F1 score and strong confidence discriminability of 0.81 in AUROC (Area Under the Receiver Operating Characteristics). Furthermore, we have implemented ELESON on mobile phones, and demonstrate that it runs in real time with low computational overhead, requires only 9MB memory usage, and consumes less than 2% battery for an operation of 2.5 hours.

The remainder of this paper is organized as follows. We first review related work in Section 2. Then, we define the problem, the causal feature extractor, and magnetic feature extractor in Section 3. We present the evidential state classifier to estimate state confidence in Section 4. We discuss experimental results in Section 5, and conclude in Section 6.

2 RELATED WORK

To our knowledge, the literature has not carefully studied the classification of pedestrian conveyor state. On the other hand, much work has been done on the recognition of various pre-defined pedestrian behaviors using the accelerometer and gyroscope of smartphones, wristbands or wearables. These include gesture recognition, human action recognition, gait detection and fall detection [7, 11–13]. Simple human actions such as standing and walking can be recognized by handcrafted features [14–18], while the more complex ones, such as gestures and sports actions, may be classified using deep learning models [19–23]. These works classify actions by processing INS signals as a whole, assuming that pedestrian is the only factor affecting the motion signals of acceleration and angular velocity. In contrast, the motion signals of the conveyor state under our consideration is a superposition of both conveyor transport and arbitrary pedestrian motion that is largely independent of the conveyor state. Therefore, these previous works struggle in our case and cannot be satisfactorily extended to our problem. Some other works tackle signal perturbations by labeling each of the actions in the training process [20, 24–30]. However, they cannot be applied to our work because precisely and exhaustively annotating the plethora of all the possible random human motions is impossible or unrealistic. In summary, this is the first piece of work on conveyor state classification without any need for pedestrian motion labeling.

Using magnetometer to extract magnetic features has been widely used for indoor localization (see, for example, [31–33] and references therein). While the issue has been mainly on extracting relevant features and matching them with a magnetic fingerprint database, we consider a different objective of using magnetic features to classify conveyor state without any fingerprint database. As the problem and setting is fundamentally different, we propose an approach to exploit the distinguishing characteristics of magnetic features between moving enclosed elevator and open escalator, so as to differentiate the states more effectively. In the process, the pedestrian location is neither known nor needs to be estimated.

Many research works have considered evidential classification for image classification, sound recognition, LiDAR/infrared object detection, etc. [34–38]. Despite the volume of work, the evidential model for INS signals is rarely studied. In this paper, we design an evidential state classifier based on the temporal feature of the conveyor states in motion and magnetic signals and present a state-evidence loss function, which enables sound classification based on confidence.

3 FEATURE EXTRACTION

In this section, we discuss how to extract reliable deep feature of the conveyor state. After defining the problem in Section 3.1, we introduce the causal feature extractor for state classification based on the motion signals of acceleration and angular velocity in Section 3.2, followed by the magnetic feature extractor to boost classification effectiveness in Section 3.3.

3.1 Problem Definition

Given a sequence of INS signals sampled from a pedestrian’s phone, denoted as $x \in \mathbb{R}^{T \times 9}$, our overarching goal is to learn a deep learning model to estimate the *conveyor state* of the pedestrian, denoted as s , which is either elevator, escalator or neither. To achieve this, the most straightforward way is learning a deep classifier that maps INS signals to the conveyor state from a labeled training dataset, assuming that the INS signals of the test are independent and identically distributed (I.I.D.) with the training dataset, i.e.

$$P(x_{test} | s) = P(x_{train} | s), \quad (1)$$

where x_{test} and x_{train} refer to the INS signals in the test and training scenarios, respectively.

However, the distribution of INS signals depends not only on the conveyor state of the pedestrian but also on the *pedestrian’s motion* and the *surrounding environment* (defined as the factors that influence the phone’s surrounding magnetic field, such as the architectural structure and metal decorations, excluding the conveyors). Specifically, pedestrian often arbitrarily and flexibly exhibit various motions to move and rotate the phone, and the diverse environments differentiate the magnetic fields surrounding the elevators and escalators at different locations. As such, we present the realistic distribution of a sequence of INS signals as

$$P(x | s, V_p, V_e), \quad (2)$$

where V_p and V_e are the variables representing the pedestrian motion and surrounding environment, respectively (the details of the two variables will be discussed later). Since these two factors often arbitrarily vary in the training and test scenarios, they lead to significant discrepancies in the INS signal distribution and violate the I.I.D. assumption of the deep classifier. Consequently, the classifier that directly learns from a training dataset could be unreliable and inaccurate in practice.

To avoid the two factors confusing the classification regarding conveyor state, we aim to reduce the distribution shift of the INS signals between training and test scenarios in deep feature space. Specifically, we extract a *conveyor state feature*, denoted as z , that is statistically independent of the pedestrian motion (V_p) and the surrounding environment (V_e), which is presented as

$$P(z | s, V_p, V_e) = P(z | s). \quad (3)$$

After this, we use the conveyor state feature for classification.

As shown in Figure 1, we divide a sequence of INS signals into the motion signals (of acceleration and angular velocity) and magnetic field signal, i.e.

$$x = [x_m, x_b], \quad (4)$$

where $x_m \in \mathbb{R}^{T \times 6}$ represents a sequence of motion signals, $x_b \in \mathbb{R}^{T \times 3}$ represents a sequence of magnetic signals, and $[\cdot, \cdot]$ stands for the concatenation operation. Based on the different signal characteristics, we extract the *conveyor causal feature* from motion signals, denoted as z_c , and the *conveyor magnetic feature* from magnetic signals, denoted as z_b . The two features are concatenated as the conveyor state feature, i.e.

$$z = [z_c, z_b], \quad (5)$$

which is used for conveyor state classification.

Next, we introduce the design of the causal feature extractor and magnetic feature extractor.

3.2 Causal Feature Extractor

3.2.1 Overview. In practice, pedestrians often consciously or unconsciously affect the motion signals on their phones, whether using an elevator/escalator or not. As a result, pedestrian’s motion entangles with the conveyor

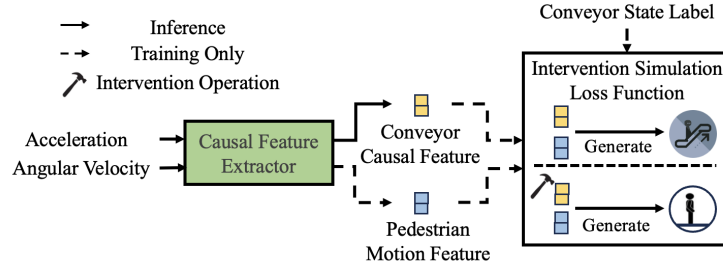


Fig. 2. Causal feature extractor disentangles conveyor state from pedestrian motion by a causal decomposition, learned from a novel intervention simulation loss function. The key idea of the loss function is to simulate an intervention operation in deep feature space.

state in motion signals and perturbs the signal patterns of the states. Formally, we present their entanglement in a sequence of motion signals (x_m) by a generation function, i.e.

$$G_m(s, V_p, V_u) = x_m, \quad (6)$$

where the motion signal pattern is mainly determined by the conveyor state (s) and pedestrian motion (V_p), and we use the variable V_u to represent the unobserved and insignificant factors to ensure the rigor of the equation.

To reduce the adverse impact of the pedestrian’s motion, we aim to *disentangle the conveyor state from the pedestrian motion in motion signals*. However, the disentanglement is challenging to achieve. First, the generation mechanism of motion signals (shown in Equation 6) is complex and intractable, making it hard to invert the generation process. Second, as pedestrian’s motion is diverse, flexible and arbitrary, it is difficult to enumerate or annotate those motions.

To achieve this disentanglement, our key idea is to learn a deep model that conducts a *causal decomposition* on the motion signal in deep feature space. Specifically, we decompose the motion signals into two deep features that separately encode the information about the conveyor state and pedestrian’s motion. Then, we use the feature of the conveyor state for classification, independent of the pedestrian’s motion.

As shown in Figure 2, we use a causal feature extractor, denoted as $f_{\theta_m}(\cdot)$, to decompose a sequence of motion signals (x_m) into a conveyor causal feature (z_c) and a pedestrian motion feature, denoted as z_p , i.e.

$$f_{\theta_m}(x_m) = [z_c, z_p], \quad (7)$$

where z_c encodes the information of the conveyor states and is used for state classification. In the implementation, for computational efficiency, the causal feature extractor empirically uses a two-layer ConvLSTM and two fully connected layers (with ReLU as the activation function) to account for the temporal feature of the conveyor states, while other temporal models should also be suitable [9]. To learn the decomposition, we propose an intervention simulation loss function based on the *causal feature* of elevator and escalator.

In the following, we introduce the causal decomposition for conveyor state classification. In Section 3.2.2, we answer the question to: *What is the causal feature of elevator and escalator?* In Section 3.2.3, we introduce: *How to practically extract the causal feature of the conveyors?*

3.2.2 Causal feature of elevator and escalator. The causal feature of an object reflects the physical property of the object. To name a classic example, temperature generally drops as altitude goes up. As the law of physics universally holds in most cases, causal feature is typically more reliable and independent of other factors to reflect an object than a statistical feature.

In our work, we identify that the *motion impact caused by transportation* is the causal feature of elevator and escalator. As long as elevator and escalator transport pedestrians (and their phones), such transportation inevitably generates unique motion impacts on motion signals. Conversely, the motion impact would not exist without the transportation of elevator or escalator. Moreover, the motion impact of transportation is naturally independent of pedestrian motion, as their existence depends only on the elevator and escalator.

To capture the motion impact of transportation, the most straightforward way is through the interventional experiment. Formally, the experiment is presented as

$$\Delta x_m = G_m(s, V_p, V_u) - G_m(N, V_p', V_u') \quad (8)$$

where $V_p = V_p'$, $V_u = V_u'$, s is either elevator or escalator state, and N stands for the neither state. In other words, the interventional experiment collects motion signals in pairs, regarding the conveyor state as the univariate and strictly controlling the other variables. In this way, the signal difference vector (Δx_m) reflects the motion impact of transportation, i.e. the causal feature of elevator and escalator.

The interventional experiment implies a causal decomposition on the motion signal. In Equation (8), by moving the second term to the other side, the decomposition is shown as

$$G_m(s, V_p, V_u) = \Delta x_m + G_m(N, V_p, V_u), \quad (9)$$

where it decomposes the signal $x_m = G_m(s, V_p, V_u)$ to the two terms on the right hand side. This decomposition is causal because it captures the signal difference Δx_m . In other words, if the conveyor state variable s is elevator or escalator, the signal difference reflects the motion impact due to the conveyor; if s is the neither state, the signal difference would be a zero vector, indicating no conveyor.

This decomposition can capture the causal feature of the elevator and escalator, independent of the pedestrian motion. In the ideal situation, given the interventional data with various pedestrian motions and conveyors, we can learn the causal decomposition by a causal feature extractor, i.e. $f_{\theta_m}(x_m) = [z_c, z_p]$ (in Equation 7), where the conveyor causal feature z_c encodes Δx_m , and the pedestrian motion feature z_p encodes $G_m(s = 0, V_p, V_u)$. Note that, we refer to z_p as the pedestrian motion feature because, in the absence of an elevator and escalator, the pedestrian's motion is the only dominant factor determining the motion signal pattern.

Unfortunately, the univariate control of the interventional experiment is extremely demanding, making it impractical to collect training data by large. In contrast, the observational experiment, where the signals are collected with arbitrary uncontrolled pedestrian motions on various conveyors, is much easier to conduct in reality. Therefore, to practically learn the causal decomposition from observational data, we propose an intervention simulation loss function.

3.2.3 Intervention Simulation Loss Function. We temporally simplify the notation of conveyor state variable to binary, where $s = 1$ refers to either the elevator or escalator state, and $s = 0$ refers to the neither state. Note that, this is only for simple discussion, and our goal is still to classify the three conveyor states of elevator, escalator and neither.

The causal decomposition is challenging to learn from observational data, because the observational data only have the *original signal*, i.e. $G_m(s, V_p, V_u)$, without the *contrasted signal*, i.e. $G_m(s = 0, V_p, V_u)$. To tackle this, we propose an intervention simulation loss function, which consists of three learning constraints. The key idea is to simulate the intervention operation in deep feature space.

The first constraint is that the decomposition should not cause information loss. We consider this by using the decomposed features to reconstruct the original signal. Facilitated by a signal generator, denoted as $g_{\theta_g}(\cdot)$, the *reconstruction loss function* is presented as

$$\mathcal{L}_{rec}(\theta_m, \theta_g) = \sum_{x_m \in \mathcal{D}} \text{MSE} \left(g_{\theta_g}(z_c + z_p + \sigma), x_m \right), \quad (10)$$

where \mathcal{D} represents training dataset, $\text{MSE}(\cdot, \cdot)$ is the mean squared error loss function, and $z_c + z_p$ is the vector addition between the two features. We empirically use a Gaussian noise σ to model the V_u in Equation (6). In the implementation, the signal generator can be learned together with the causal feature extractor.

Second, the decomposition of causal feature extractor should comply with how the interventional experiment segregates the motion signal. In the interventional experiment, we remove the conveyor (of elevator or escalator) and calculate the difference between the original and contrasted signals, capturing the causal feature of elevator and escalator. Formally, for the original signal collected on elevator or escalator denoted as $G_m(s = 1, V_p, V_u)$, its contrasted signal is generated by

$$G_m(\text{do}(s = 1), V_p, V_u), \quad (11)$$

where the do-calculus indicates an *intervention operation* on the conveyor state variable. Specifically, it changes the value of the conveyor variable from elevator/escalator state ($s = 1$) to the neither state ($s = 0$).

We simulate this intervention operation in deep feature space. Our intuition is: if the decomposition is causal, the resulting conveyor causal feature (z_c) and pedestrian motion feature (z_p) should separately encode Δx_m and $G_m(s = 0, V_p, V_u)$. As such, combining the two features should be able to generate the original signal, and the pedestrian motion feature alone should generate the contrasted signal, which is summarized as

$$\begin{aligned} g_{\theta_g}(z_c + z_p) &= G_m(s = 1, V_p, V_u), \\ g_{\theta_g}(z_p) &= G_m(\text{do}(s = 1), V_p, V_u), \end{aligned} \quad (12)$$

recalling that $g_{\theta_g}(\cdot)$ is the signal generator. Although we do not have the contrasted signal, at least, we know that the intervention operation has changed the elevator and escalator state to the neither state. Therefore, the pedestrian motion feature alone should generate the signals whose distribution conforms to the signals of the neither state, i.e.

$$g_{\theta_g}(z_p) \sim P(x_m | s = 0), \quad (13)$$

which serves as a loose constraint of Equation (12). To determine whether a signal conforms to a distribution, we use a classifier denoted as $k_{\theta_k}(\cdot)$. In the implementation, the classifier directly classifies in feature space instead of signal space, since the signal is generated from the feature. Overall, we implement the constraint in Equation (12) by an *intervention loss function*, i.e.

$$\mathcal{L}_{int}(\theta_m, \theta_k) = \sum_{(x_m, y) \in \mathcal{D}} [\text{CE}(k_{\theta_k}(z_c + z_p), s = y) + \text{CE}(k_{\theta_k}(z_p), s = 0)]. \quad (14)$$

where y is the conveyor state label, $\text{CE}(\cdot)$ is the cross-entropy loss function, and the classifier learns together with the feature extractor.

Third, the conveyor causal feature should be consistent. Lacking contrasted signals, we can only give a loose constraint as in Equation (13). As a result, there are still multiple ways of decomposition given the previous two loss functions, making it insufficient for learning the causal decomposition. To tackle this, we further consider the consistency of the causal feature of elevator and escalator, based on the concept of sparse mechanism shift (SMS) in causal representation learning. SMS argues that feature changes are typically sparse and localized within a causal decomposition [39]. Extending to our case, pedestrian motion should not affect the mechanism that elevator and escalator impact motion signals. We hence enforce a consistency constraint upon the conveyor causal feature by a *consistency loss function*, i.e.

$$\mathcal{L}_{con}(\theta_m) = \sum_{\{x_m | s=1\} \in \mathcal{D}} \text{MSE}(z_c, \bar{z}_c), \quad (15)$$

where \bar{z}_c is the mean vector of the conveyor causal feature separately of the elevator and escalator states over the training dataset.

Overall, we combine the three loss functions as the *intervention simulation loss function*, which is given as

$$\mathcal{L}_{Sim} = \mathcal{L}_{int} + w_1 \mathcal{L}_{rec} + w_2 \mathcal{L}_{con}. \quad (16)$$

Without losing generality, we use two weights, separately denoted as w_1 and w_2 , to represent their relative importance. In the implementation, we use the intervention simulation loss function to learn the causal feature extractor end-to-end.

3.3 Magnetic Feature Extractor

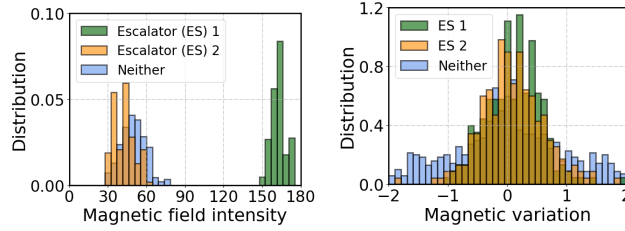


Fig. 3. Evidence that the temporal variation of the magnetic field (right) exhibits greater stability as a characteristic of the escalator state compared to the raw magnetic field signals (left).

The magnetometer samples the 3D magnetic field orientation at the phone’s location, generating a sequence of magnetic field signals over time, which is presented as

$$x_b = \left[x_b^{(0)}, x_b^{(1)}, \dots, x_b^{(T-1)} \right]. \quad (17)$$

The magnetic field signals in elevator and escalator have two features. First, the metallic material and structure of elevator and escalator affect the magnetic field environment in them. In particular, elevator creates an enclosed metallic environment, and the escalator forms a semi-open space. Second, the magnetic signal varies with the moving pedestrian in elevator and escalator.

However, magnetic field signals are noisy, making it challenging to classify the conveyor states. For one thing, since the surrounding environment (V_e) affects the magnetic field in elevator and escalator, the magnetic signal is dependent on the conveyor’s location. As shown in Figure 3 (left), the magnetic signal in the same type of conveyor can be very different by location. For another, many pedestrian motions (V_p), such as waving and rotating phones, fluctuate the magnetic field signal. Therefore, to leverage magnetic field signals for conveyor state classification, we need to extract *a stable magnetic feature of the conveyor state that is environmentally independent and robust to pedestrian motions*.

As shown in Figure 4, we propose a magnetic feature extractor consisting of a variation feature extractor and a motion filter. Specifically, the variation feature extractor extracts a *magnetic variation feature* from the raw magnetic signals, alleviating the model’s dependency on environments. After that, we employ a motion filter to reduce the noises of the pedestrian motion from the variation feature. In the training stage, the motion filter learns from a motion-adversarial loss function.

To extract a more environmentally-independent feature from magnetic field signals, we focus on the moving pattern of pedestrian in elevator and escalator. Specifically, pedestrians in the same conveyor type usually have similar moving patterns, regardless of the surrounding environment. For example, most elevators first speed up and slow down, while the pedestrian on escalator tends to have a constant moving speed. Since the signal varies as the pedestrian moves, we use the temporal variation of the magnetic signals to capture the moving pattern. As shown in Figure 3, we conduct an empirical study comparing the magnetic field intensity (1D) with the magnetic

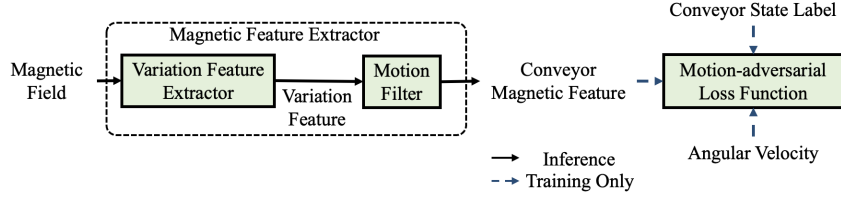


Fig. 4. System diagram of magnetic feature extractor. The variation feature extractor obtains a more environmentally independent feature of conveyor state from raw magnetic field signals. Motion filter enhances the feature robustness against pedestrian motion.

variation. In the figure, the magnetic variation can differentiate among the conveyor states and significantly reduces the environmental dependency of the raw magnetic signals. Therefore, we extract the magnetic variation feature, denoted as Δx_b , by a *variation feature extractor*, denoted as $f_b(\cdot)$, from magnetic field signals, i.e.

$$f_b(x_b) = \Delta x_b = \left[\left\| x_b^{(t+1)} \right\|_2 - \left\| x_b^{(t)} \right\|_2, t = 0, 1, \dots, T - 2 \right]. \quad (18)$$

Empirically, we find that the 1D magnetic field intensity is more effective than the 3D magnetic field orientation (as verified in Figure 16).

Nevertheless, pedestrian motions may fluctuate the phone's location and perturb the variation feature. To tackle this, our intuition is to enhance the variation feature to be insensitive to pedestrian motion. To achieve this, we propose a *motion filter*, denoted as $f_{\theta_b}(\cdot)$, to enhance the variation feature, i.e.

$$f_{\theta_b}(\Delta x_b) = z_b, \quad (19)$$

where we refer to z_b as the *conveyor magnetic feature*. Denoting pedestrian motion variable (V_p) as binary, we reduce the feature discrepancy with and without pedestrian motion, i.e.

$$\min \left\| P(z_b | s = 1, V_p = 0) - P(z_b | s = 1, V_p = 1) \right\|_n, \quad (20)$$

where $V_p = 1$ refers to that pedestrian motion perturbs magnetic signals such as waving and rotating, and $V_p = 0$ otherwise. Observing that pedestrian motion could often lead to large angular velocity while elevator and escalator cannot, we use an angular-velocity threshold to determine V_p . Given the above, we train the motion filter by a *motion-adversarial loss function*, i.e.

$$\mathcal{L}_{Adv}(\theta_b) = - \sum_{x_b \in \mathcal{D}} \text{CE} (k_{\theta_b} (f_{\theta_b}(\Delta x_b)), V_p), \quad (21)$$

where the motion filter plays a min-max game with a classifier that classifies V_p using the conveyor magnetic feature, denoted as $k_{\theta_b}(\cdot)$. Note that, the motion-adversarial loss function only enhances the robustness of the conveyor magnetic feature against the motion noise. For state classification, the motion filter learns together with the state classifier, which will be discussed in the next section.

In the implementation, we empirically use the angular-velocity threshold of 1.5 rad/s, and the motion filter consists of a two-layer ConvLSTM and two fully connected layers with ReLU as the activation function [9].

4 EVIDENTIAL STATE CLASSIFIER

After the feature extraction, ELESON employs an evidential state classifier to estimate the state confidence of pedestrians. We overview the classifier in Section 4.1, and introduce the state-evidence loss function in Section 4.2.

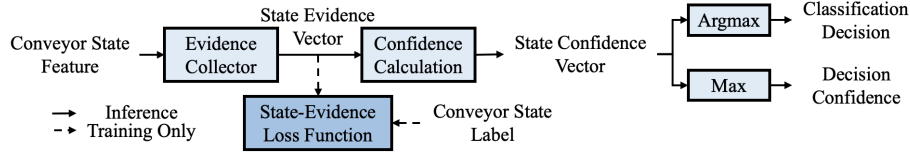


Fig. 5. System diagram of evidential state classifier. The evidence collector extracts evidence supporting the classification of the pedestrian in each of the states. The evidence is then processed through normalization to state confidence.

4.1 Overview

The duration for taking an elevator or escalator varies in practice. For instance, the time on an elevator varies by the pedestrian’s usage; and the duration for taking escalator depends on the escalator’s size and speed. On the other hand, taking elevator and escalator have many temporal patterns, e.g., an elevator has to first speed up before slowing down. Therefore, to account for the variable duration and capture the temporal patterns, we classify the conveyor state of pedestrian by short time segments (e.g., 2 seconds), based on the long-term temporal features extracted by the two feature extractors (using LSTM).

In each segment, given the conveyor state feature, we aim to classify the conveyor state and estimate the confidence behind the classification decision, denoted as c . We trust the classification decision if the confidence is larger than a threshold and remain undecided (UD) otherwise. The confidence estimation provides an opportunity to enhance the system’s reliability by discarding the less-confident decisions (as UD). Therefore, *it is important for the estimated confidence to reflect the classification accuracy effectively*.

We identify two sources of confidence in classifying the conveyor state. The first source is the signal-to-noise ratio of INS signals. For example, suppose a pedestrian exhibits a motion far more intense than the conveyor, the resulting motion signals could make it difficult to differentiate the conveyor states, leading to low confidence in the classification. The second source is the classifier’s familiarity with the target signal, given its training dataset. A classifier is usually accurate in classifying the signal in its training data and could be more error-prone when tackling unfamiliar signals (possibly caused by unseen pedestrian motions, extreme magnetic environments, unconsidered conveyor types, etc.) Even with enhanced robustness in the conveyor state feature, less familiar signals inevitably result in lower confidence.

The most common Softmax-based classifier does not consider its familiarity with the input signal and thus is often overconfident about its decision [40, 41]. Existing confidence estimation frameworks that account for the two sources are mainly based on the Bayes method and evidence theory. In this paper, we build an *evidential state classifier* based on evidence theory, leveraging its computational efficiency on smartphones. Specifically, the evidential state classifier can effectively estimate the state confidence, being as computationally efficient as the Softmax-based classifier.

The system diagram of the evidential state classifier is illustrated in Figure 5. Given a conveyor state feature (z), the classifier first extracts a *state evidence vector*, denoted as E , using an *evidence collector*, denoted as $f_{\theta_e}(\cdot)$, i.e.

$$f_{\theta_e}(z) = E, \quad (22)$$

where $\{e_s \mid e_s \in E, e_s \geq 0\}$ is the *evidence value* supporting the conveyor state s , and $\dim(E) = 3$. After that, we calculate the *state confidence vector*, denoted as C , using the state evidence vector by

$$C = \frac{E}{e_u + \sum_{e \in E} e}, \quad (23)$$

where $\{c_s \mid c_s \in C, c_s \in [0, 1]\}$ is the confidence of state s , e_u is the *uncertainty constant*, and we empirically set it to $e_u = \dim(E)$. We select the state with the highest confidence as the classification decision, which is given as

$$s^* = \arg \max_{c \in C} c. \quad (24)$$

Finally, if the highest confidence is larger than a threshold, i.e. $\max(C) > \tau$, we trust the classification decision. Otherwise, the system outputs “undecided” (UD).

In the implementation, the evidence collector consists of three fully connected layers. We use ReLU as the activation function as well as the output layer to guarantee that $e_s \geq 0$. The evidence collector is expected to extract evidence reflecting the two sources of confidence. To achieve this, we propose a state-evidence loss function in the training stage. The loss function supervises the classifier to estimate the state confidence using the temporal feature of conveyor states.

4.2 State-evidence Loss Function

Since a pedestrian can either be on an elevator, escalator or neither, the probabilities of the three states sum up to one. However, considering that the classifier may not be familiar with the input signal, we additionally use an uncertainty term to occupy a fraction of the probability. The uncertainty term indicates the “equal likely” of the three states due to the unfamiliarity of input signals. By considering the uncertainty term, the probability assignment becomes subjective to the training data of the classifier. Therefore, the probability assigned to each of the conveyor states ($c_s \in C$) is called the *state confidence*. Formally, the uncertainty term, denoted as u , forms a 3-simplex with the three state confidence, which is shown as

$$u + \sum_{c_s \in C} c_s = 1. \quad (25)$$

In evidence theory, confidence is supported by the quantity of evidence. If the classifier has sufficient evidence to support a decision, it would be less uncertain. Recalling that E is the state confidence vector, and $e_u (= \dim(E))$ is the uncertainty constant, the uncertainty term can be quantified as

$$u = \frac{e_u}{e_u + \sum_{e \in E} e}. \quad (26)$$

Based on the evidence value, the state confidence vector (C) is calculated as in Equation (23).

We learn an evidence collector to estimate the evidence value of each state, i.e. $f_{\theta_e}(z) = E$ in Equation (22). The first objective of the evidence collector is *to classify the conveyor states as accurately as possible*, which is identical to the goal of the Softmax-based classifier. To achieve this, recalling that x denotes a sequence of INS signals, $CE(\cdot, \cdot)$ is the cross-entropy loss function, and y is the conveyor state label, we use an evidence classification (EC) loss function, i.e.

$$\mathcal{L}_{EC}(\theta_m, \theta_b, \theta_e) = \sum_{(x,y) \in \mathcal{D}} CE\left(\frac{E}{\sum_{e \in E} e}, y\right), \quad (27)$$

which trains both feature extractors and the evidence collector. Similar to the Softmax classifier, this reflects the first source of confidence.

The second objective is *to reduce the uncertainty in classifying familiar input signals*. Regarding familiarity as the frequency of the classifier seeing a signal, we gradually reduce the uncertainty as the signal appears more frequently in the training data. Specifically, the 3-simplex in Equation (25) can be transformed into a Dirichlet distribution whose variance is proportional to the uncertainty term (proof is in [41]). Denoting $a_s = e_s + 1$ and $A = \sum_{e \in E} (e + 1)$, the variance of the transformed Dirichlet distribution is presented as

$$\text{Var}(E) = \sum_s \frac{a_s(A - a_s)}{A^2(A + 1)}. \quad (28)$$

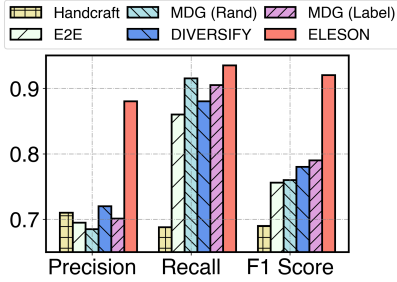


Fig. 6. ELESON significantly outperforms existing methods, achieving an approximate 14% improvement in F1 score.

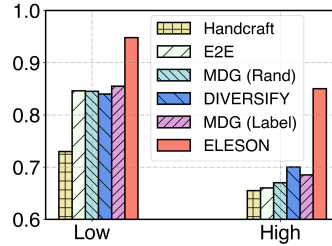


Fig. 7. ELESON attains a satisfactory F1 score exceeding 0.85 under both low and high levels of pedestrian motions.

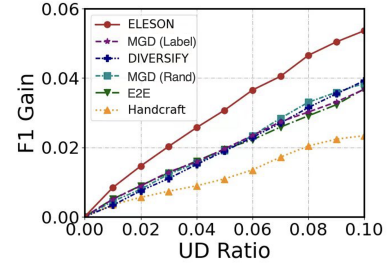


Fig. 8. ELESON benefits higher F1 score from the same UD ratio due to confidence estimation, achieving 3% improvement with 0.05 UD ratio.

Therefore, we directly minimize the variance of the Dirichlet distribution to reduce its uncertainty for the signals in training data. Overall, we learn the evidence collector by a *state-evidence loss function*, which is given as

$$\mathcal{L}_{SE} = \mathcal{L}_{EC} + \sum_{\mathcal{D}} \text{Var}(E). \quad (29)$$

In the implementation, we learn both feature extractors and the classifier end-to-end. Recalling that \mathcal{L}_{Adv} is the motion-adversarial loss function in Equation (21), and \mathcal{L}_{Sim} is the counterfactual simulation loss function in Equation (16), the loss function for training the whole system is given as

$$\mathcal{L} = \mathcal{L}_{SE} + w_3 \mathcal{L}_{Adv} + w_4 \mathcal{L}_{Sim}, \quad (30)$$

where w_3 and w_4 represent the relative importance among the three loss functions.

5 ILLUSTRATIVE EXPERIMENTAL RESULTS

In this section, we evaluate the performance of ELESON. We first discuss the experimental settings in Section 5.1, and then show ELESON’s performance in Section 5.2, verify system parameters in Section 5.3, and study the computing efficiency in Section 5.4.

5.1 Experimental Setting

We collect real pedestrian data to verify ELESON. In data collection, each pedestrian walked around a shopping mall, casually carried his/her phone in any style and motion and took different elevators and escalators in the process. Meanwhile, an observer annotated the pedestrian’s conveyor state, phone carriage styles, and the timestamps when it got on and off a conveyor. Overall, we collected the conveyor state data from 15 persons and 10 shopping malls over 20 hours (roughly 20% in elevators, 20% on escalators, and 60% are neither). To our knowledge, this is the first dataset for classifying the conveyor states of pedestrians.

Considering that the pedestrians used elevators and escalators for varied time lengths, we classify the conveyor state using a sliding window with size and stride of 2 seconds. To balance the state label, borrowing from object detection, we evaluate ELESON by computing F1 score individually for elevator and escalator states based on the classification results, which is given as

$$\text{F1 score} = \frac{2 \times \text{Precision} \times \text{Recall}}{\text{Precision} + \text{Recall}}. \quad (31)$$

Specifically, precision and recall are the proportions of true positives separately over predicted positives and actual positives, i.e. Precision = $TP/(TP + FP)$, Recall = $TP/(TP + FN)$, where TP, FP, and FN stand for “true positive”, “false positive”, and “false negative”. Unless particularly specified, we report the sum of the F1 scores of elevator and escalator states.

We compare ELESON with the following classification approaches on INS signals:

- *Handcrafted feature approach (Handcraft)* [42] designs handcrafted features (mean and variance, etc.) on motion and magnetic signals. For fairness, we use a neural network to classify conveyor states based on those features.
- *End-to-end Approach (E2E)* [9] is our backbone approach. It classifies INS signals using ConvLSTM end-to-end.
- *Multi-domain Generalization (MDG)* [29] enhances feature robustness using labels on human motions. In the experiment, we label human motions using random labels (Rand) and phone carriage styles (Label), as in Table 1, and classify conveyor states using ConvLSTM.
- *DIVERSIFY* [27] is a single-domain generalization approach. It reduces the feature variance in training data based on a clustering algorithm. In the experiment, we use ConvLSTM to classify conveyor states incorporating the scheme.

We verify confidence estimation by the area under the receiver operating characteristic curve (AUROC), which measures the discriminability of confidence to distinguish correct and false classification results. We regard it as a true positive case when a false result is regarded as UD. Formally, AUROC measures the trade-off between false positive rate and true positive rate, which is computed as

$$\text{AUROC} = \int_0^1 S_{\mathcal{D}}(r) dr, \quad (32)$$

where r is the false positive rate and $S_{\mathcal{D}}(r)$ maps r to the true positive rate given a dataset \mathcal{D} . We compare confidence estimation with the following approaches:

- *Entropy approach (Softmax)* [43] uses information entropy of the classification score to presents the confidence of Softmax-based classifier;
- *Bayesian neural network (Bayesian)* [44] represents confidence using prediction variance over network parameter’s distribution. In the experiment, we sample network parameter by Dropout mechanism [43];
- *Temperature scaling (TempScale)* [45] calibrates the classification scores using an exponential parameter, calibrated in training data, and calculates confidence using the information entropy of the scores.

Additionally, we have verified ELESON’s on-device performance by deploying it to an Android phone (Huawei LDN-AL10), investigating its power consumption, memory usage and inference time. This is shown in Section 5.4.

In the experiment, ELESON is optimized by Adam optimizer end-to-end. Unless particularly specified, the modules mentioned in Section 3 and 4 are four fully connected layers with ReLU functions. The conveyor causal feature and conveyor magnetic feature are 128-dimension. We use five-fold cross-validation to verify the results, randomly shuffling the sequences of INS signals by each collection.

5.2 System Performance

Figure 6 compares ELESON with the state-of-the-art (SOTA) schemes based on the confidence threshold of 0.5 (leading to 5% UD ratio). From the figure, the handcrafted feature approach performs the worst because those features are not flexible enough, thus necessitating the deep learning approach for conveyor state classification. The other schemes cannot balance precision and recall due to the arbitrary pedestrian motions and noisy magnetic environments. In comparison, ELESON achieves satisfied results on recall and precision by extracting the conveyor causal and magnetic features. Besides, by 0.05 UD ratio, ELESON has gained around 3% F1 score improvement. Overall, ELESON achieves 0.92 of F1 score, outperforming SOTA schemes by around 14%.

Carriage style	Reading	In-pocket	Swing	In-bag
Handcraft	0.73	0.66	0.69	0.60
E2E	0.76	0.76	0.68	0.77
MDG (Rand)	0.79	0.75	0.71	0.73
DIVERSIFY	0.79	0.75	0.72	0.78
MDG (Label)	0.81	0.78	0.73	0.78
ELESON	0.92	0.92	0.84	0.88

Table 1. F1 score for various phone carriage styles at a UD ratio of 0.

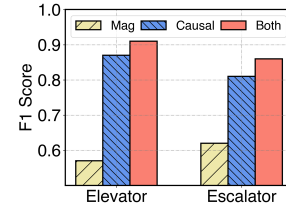


Fig. 9. Ablation study on conveyor causal and magnetic features at a UD ratio of 0.

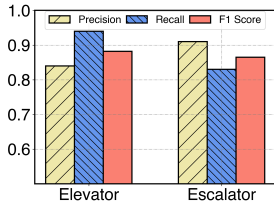


Fig. 10. ELESON’s performance on unseen elevators and escalators.

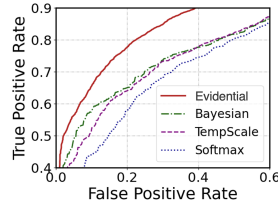


Fig. 11. ROC of state confidence estimation.

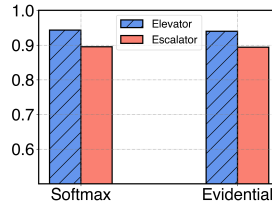


Fig. 12. Evidential state classifier shows comparable accuracy to Softmax-based classifier.

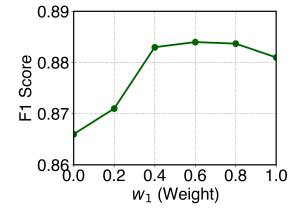


Fig. 13. F1 score versus the weight of reconstruction loss function.

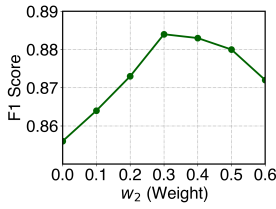


Fig. 14. F1 score versus the weight of consistency loss function.

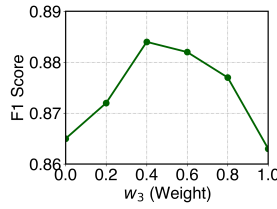


Fig. 15. F1 score versus the weight of motion-adversarial loss function.

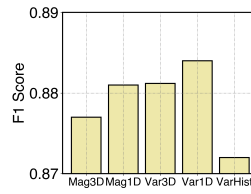


Fig. 16. Study on variation feature extractor.

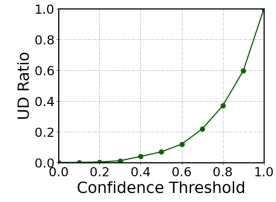


Fig. 17. UD ratio versus confidence threshold.

Figure 7 demonstrates ELESON’s performance under low and high levels of pedestrian motions. Similar to Section 3.3, we use an intensity threshold of 1.5 rad/s on angular velocity to differentiate the levels of motion perturbation. From the figure, since intense pedestrian motion reduces the signal-to-noise ratio of signals, the performance of all schemes, including ELESON, degrades in the high levels of perturbations. Despite this, ELESON demonstrates high F1 scores over 0.85 in both scenarios, verifying its stability under human perturbations.

Figure 8 shows how F1 score varies with the UD ratio (by changing the confidence threshold). The comparison schemes use Softmax-based classifier as their original setting. Being sensitive to unfamiliar signals, ELESON gains more improvement in F1 score given the same UD ratio, achieving 3% improvement under only UD ratio of 0.05. This verifies that the confidence estimation of ELESON can further enhance the system’s reliability.

Table 1 compares the F1 scores of the schemes for different phone carriage styles. This is a coarse but explainable way to label pedestrian motions. From the table, the schemes performs relatively better in stable carriage styles

(such as reading) than dynamic styles (such as swinging). Note that, ELESON outperforming MDG (Label) verifies that the causal decomposition is more effective than using the coarse labels of pedestrian motion. Overall, ELESON shows superior F1 scores in all carriage styles, which is consistent with the previous results.

Figure 9 shows an ablation study on the conveyor causal feature and conveyor magnetic feature, with a UD ratio of 0. From the figure, the causal feature majorly contributes to the F1 score, and the magnetic feature further boosts the classification accuracy, because they characterize the conveyor state of pedestrians from different aspects. Additionally, the figure shows that elevator has higher F1 score than escalator. This is because pedestrian in elevator usually performs fewer motions than on escalator, leading to higher signal-to-noise ratio. Also, the acceleration pattern on elevator is more distinguishable from the neither state, making them less confused.

Figure 10 demonstrates ELESON’s performance on unseen elevators and escalators. In this experiment, we separate training and testing data by shopping malls in the five-fold cross-validation, such that the conveyors in test are unseen to the model. In the figure, ELESON’s F1 score slightly degrades by around 3–4% compared with previous results, due to the subtle shifts of motion patterns and magnetic environments of the conveyors. Despite so, with the enhanced feature robustness, ELESON achieves satisfying F1 scores (more than 0.85) on unseen elevators and escalators. This validates ELESON’s applicability in practice.

Figure 11 compares different confidence estimation approaches for conveyor state classification using ROC curve, given the two feature extractors. The curve indicates a better discriminability of confidence when it is closer to the upper-left corner. In the figure, the entropy-based approach (Softmax) is overconfident and suffers poor discriminability. The temperature scaling (TempScale) reduces Softmax’s confidence universally, thus leading to limited improvement. Bayesian approach is unstable due to its sampling nature (while more samples lead to heavy computations). Overall, the evidential state classifier achieves strong confidence discriminability 0.81 in AUROC, outperforming the other schemes by a large margin.

Following Figure 11, Figure 12 compares the classification effectiveness between the evidential state classifier and Softmax-based classifier. The figure shows a comparable F1 score of the evidential state classifier with the Softmax-based classifier, due to the evidence classification loss function in Equation (27). This verifies that the evidential state classifier can achieve better confidence estimation without compromising classification accuracy.

5.3 Study on System Parameters

In this section, we verify ELESON’s system parameter using the UD ratio of 0.

Figure 13 shows how ELESON’s performance varies with the weight of reconstruction loss function (in Equation 10). From the figure, the F1 score increases with the weight when it is less than 0.4 and flats off after that. The gain is because the reconstruction loss function reduces the information loss of the decomposition. In the experiment, we use $w_1 = 0.6$.

Figure 14 demonstrates how F1 score varies with the weight of the consistency loss function (in Equation 15). In the figure, the accuracy shows a U-shape as the weight increases. The increase of F1 score is because the consistency loss function stabilizes the causal feature. The decrease, on the other hand, is when the weight is so large that the extracted features are inflexible. In the experiment, we use $w_2 = 0.3$.

Figure 15 shows how F1 score varies with the weight of the motion-adversarial loss function (in Equation 21). Similar to Figure 14, the accuracy shows a U-shape varying with the weight. The accuracy increases because the motion filter enhances the variation feature robust against pedestrian motions. However, stressing too much on adversarial learning may cause the feature to be inflexible. In the experiment, we use $w_3 = 0.4$.

Figure 16 studies the different implementations of the variation feature extractor in Equation (19). Specifically, “Mag3D” stands for the 3D magnetic field signal, “Mag1D” is the magnetic field intensity, “Var3D” is the 3D magnetic variation, “Var1D” is the 1D magnetic variation, and “VarHist” is the histogram of magnetic variation. As mentioned, the variation feature is better than the raw magnetic field signals because it is more environmentally

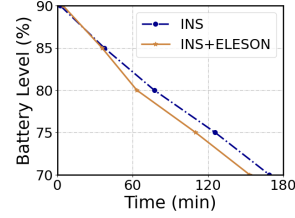
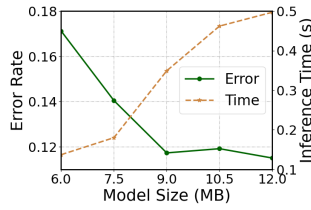


Fig. 18. Inference time and error versus model size. Fig. 19. Study on ELESON’s power consumption.

independent. The 3D signal introduces the noisy phone pose information, which is irrelevant to conveyor states, making it worse than 1D signal features. The “VarHist” performs the worst because it reduces the temporal feature of conveyors.

Figure 17 shows the confidence distribution of ELESON in testing (over the whole dataset). The figure shows that the UD ratio grows exponentially with confidence threshold, showing a short tail on the left side. It indicates that ELESON is confident about most of the testing signals. In the experiment, we set the confidence threshold as 0.5, which leads to a UD ratio of 5%.

5.4 Efficiency Study

Figure 18 shows how the error rate and inference time (by making one prediction) vary with model size. We adjust the model size by changing the neuron quantity of each layer, and error rate is calculated by one minus the F1 score. In the figure, the inference time naturally increases with model size, while the error rate reduces in the beginning and knees down at the model size of 9MB. Therefore, we choose the model size of 9MB, which is around 0.3% of the phone’s memory, when each model inference takes around 0.4 seconds. With this setting, ELESON can operate in real-time (inference time is less than 2 seconds) with minimal memory and satisfying accuracy.

Figure 19 demonstrates the power consumption by running ELESON on a smartphone. In the experiment, we turn on the INS sensor and use ELESON to process the INS signals. In the contrasted group, we keep the same phone status and turn on the INS sensor without running ELESON. From the figure, INS consumes around 18% of the battery levels (from 90% to 72%) in 150 minutes, and additionally running ELESON only takes 2% more battery in the same period, which is even trivial compared with the INS sensor. This shows ELESON’s minimal computational cost in terms of power consumption.

6 CONCLUSION

We study, for the first time, how to classify a pedestrian in one of the three conveyor states of elevator, escalator and neither, given the INS readings of acceleration, angular velocity and magnetic fields sampled from the pedestrian’s phone. This problem is challenging because arbitrary pedestrian motions and diverse magnetic environments perturb the INS signals of conveyor states, which confuses previous classification approaches once extended to this problem. We propose ELESON, a novel, effective and lightweight INS-based deep learning approach to classify pedestrian’s conveyor states of elevator, escalator or neither. ELESON utilizes a causal feature extractor to disentangle the conveyor state from pedestrian motion based on causal decomposition and employs a magnetic feature extractor to explore the unique magnetic field characteristics of elevator and escalator. After feature extraction, it uses an evidential state classifier to estimate the state confidence of pedestrians. We have conducted experiments to validate ELESON on over twenty hours of real pedestrian data and compared it with state-of-the-art classification approaches. Our results show that ELESON significantly outperforms prior arts by

14% in F1 score, with a strong confidence discriminability of 0.81 in AUROC. Furthermore, we have implemented ELESON on Android devices, where it operates in real-time, achieving 0.4s for one model inference, requiring only 9MB memory usage and consuming 2% battery in 2.5 hours.

As a pioneering work in classifying the conveyor states of pedestrians, ELESON provides valuable insights into recognizing various types of pedestrian conveyor states, such as pedestrians on travelators, wheelchairs, and self-balancing scooters. These applications hold significant potential in human-machine interaction, Internet of Things, and smart cities. In the future, we will explore the adaptation of ELESON to additional conveyor types with a focus on data efficiency, enabling the knowledge transfer across classifying different conveyor states while minimizing data collection efforts. Besides, another future orientation is to infer the direction and levels of floor transition based on ELESON's feature extractors, which provides more fine-grained information for indoor navigation. Such information may be extracted in an unsupervised manner with an effective clustering algorithm from the conveyor state features.

REFERENCES

- [1] J. Wang, Z. Zhao, M. Ou, J. Cui, and B. Wu, "Automatic Update for Wi-Fi Fingerprinting Indoor Localization via Multi-Target Domain Adaptation," *Proceedings of the ACM on Interactive, Mobile, Wearable and Ubiquitous Technologies*, vol. 7, no. 2, pp. 1–27, 2023.
- [2] X. Yang, S. He, B. Wang, and M. Tabatabaie, "Spatio-Temporal Graph Attention Embedding for Joint Crowd Flow and Transition Predictions: A Wi-Fi-based Mobility Case Study," *Proceedings of the ACM on Interactive, Mobile, Wearable and Ubiquitous Technologies*, vol. 5, no. 4, pp. 1–24, 2021.
- [3] H. Ma, Y. He, M. Li, N. Patwari, and S. Sigg, "Introduction to the Special Issue on Wireless Sensing for IoT," *ACM Transactions on Internet of Things*, vol. 33, no. 2, pp. 1–4, 2023.
- [4] W. Zhuo, K. H. Chiu, J. Chen, Z. Zhao, S.-H. G. Chan, S. Ha, and C.-H. Lee, "FIS-ONE: Floor Identification System with One Label for Crowdsourced RF Signals," in *2023 IEEE 43rd International Conference on Distributed Computing Systems (ICDCS)*. IEEE, 2023, pp. 418–428.
- [5] T. Zhang, D. Zhang, G. Wang, Y. Li, Y. Hu, Q. Sun, and Y. Chen, "Rloc: Towards Robust Indoor Localization by Quantifying Uncertainty," *Proceedings of the ACM on Interactive, Mobile, Wearable and Ubiquitous Technologies*, vol. 7, no. 4, pp. 1–28, 2024.
- [6] T. He, J. Tan, and S.-H. G. Chan, "Self-supervised Association of Wi-Fi Probe Requests under MAC Address Randomization," *IEEE Transactions on Mobile Computing*, vol. 22, no. 12, pp. 7044–7056, 2022.
- [7] W. Zhang, H. Dai, D. Xia, Y. Pan, Z. Li, W. Wang, Z. Li, L. Wang, and G. Chen, "mP-Gait: Fine-grained Parkinson's Disease Gait Impairment Assessment with Robust Feature Analysis," *Proceedings of the ACM on Interactive, Mobile, Wearable and Ubiquitous Technologies*, vol. 8, no. 3, pp. 1–31, 2024.
- [8] J. Lu and K.-Y. Tong, "Robust Single Accelerometer-based Activity Recognition Using Modified Recurrence Plot," *IEEE Sensors Journal*, vol. 19, no. 15, pp. 6317–6324, 2019.
- [9] Y. A. Andrade-Ambriz, S. Ledesma, M.-A. Ibarra-Manzano, M. I. Oros-Flores, and D.-L. Almanza-Ojeda, "Human Activity Recognition Using Temporal Convolutional Neural Network Architecture," *Expert Systems with Applications*, vol. 191, p. 116287, 2022.
- [10] H. Xu, P. Zhou, R. Tan, and M. Li, "Practically Adopting Human Activity Recognition," in *Proceedings of the 29th Annual International Conference on Mobile Computing and Networking*, 2023, pp. 1–15.
- [11] D. Zhang, Z. Liao, W. Xie, X. Wu, H. Xie, J. Xiao, and L. Jiang, "Fine-grained and Real-time Gesture Recognition by Using IMU Sensors," *IEEE Transactions on Mobile Computing*, 2021.
- [12] H. Prasanth, M. Caban, U. Keller, G. Courtine, A. Ijspeert, H. Vallery, and J. Von Zitzewitz, "Wearable Sensor-based Real-time Gait detection: A Systematic Review," *Sensors*, vol. 21, no. 8, p. 2727, 2021.
- [13] X. Chen, S. Jiang, and B. Lo, "Subject-independent Slow Fall Detection with Wearable Sensors via Deep Learning," in *2020 IEEE SENSORS*. IEEE, 2020, pp. 1–4.
- [14] Z. Yang, C. Wu, Z. Zhou, X. Zhang, X. Wang, and Y. Liu, "Mobility Increases Localizability: A Survey on Wireless Indoor Localization Using Inertial Sensors," *ACM Computing Surveys (Csur)*, vol. 47, no. 3, pp. 1–34, 2015.
- [15] E. Bulbul, A. Cetin, and I. A. Dogru, "Human Activity Recognition Using Smartphones," in *2018 2nd International Symposium on Multidisciplinary Studies and Innovative Technologies (ISMSIT)*. IEEE, 2018, pp. 1–6.
- [16] A. Brajdic and R. Harle, "Walk Detection and Step Counting on Unconstrained Smartphones," in *Proceedings of the 2013 ACM International Joint Conference on Pervasive and Ubiquitous Computing*, 2013, pp. 225–234.
- [17] X. Kang, B. Huang, and G. Qi, "A Novel Walking Detection and Step Counting Algorithm Using Unconstrained Smartphones," *Sensors*, vol. 18, no. 1, p. 297, 2018.

- [18] F. Demrozi, G. Pravadelli, A. Bihorac, and P. Rashidi, “Human Activity Recognition Using Inertial, Physiological and Environmental Sensors: A Comprehensive Survey,” *IEEE access*, vol. 8, pp. 210 816–210 836, 2020.
- [19] Z. Hong, Z. Li, S. Zhong, W. Lyu, H. Wang, Y. Ding, T. He, and D. Zhang, “CrossHAR: Generalizing Cross-dataset Human Activity Recognition via Hierarchical Self-Supervised Pretraining,” *Proceedings of the ACM on Interactive, Mobile, Wearable and Ubiquitous Technologies*, vol. 8, no. 2, pp. 1–26, 2024.
- [20] S. Miao, L. Chen, and R. Hu, “Spatial-Temporal Masked Autoencoder for Multi-Device Wearable Human Activity Recognition,” *Proceedings of the ACM on Interactive, Mobile, Wearable and Ubiquitous Technologies*, vol. 7, no. 4, pp. 1–25, 2024.
- [21] M. A. Khatun, M. A. Yousuf, S. Ahmed, M. Z. Uddin, S. A. Alyami, S. Al-Ashhab, H. F. Akhdar, A. Khan, A. Azad, and M. A. Moni, “Deep CNN-LSTM with Self-attention Model for Human Activity Recognition Using Wearable Sensor,” *IEEE Journal of Translational Engineering in Health and Medicine*, vol. 10, pp. 1–16, 2022.
- [22] H. Haresamudram, I. Essa, and T. Plötz, “Contrastive Predictive Coding for Human Activity Recognition,” *Proceedings of the ACM on Interactive, Mobile, Wearable and Ubiquitous Technologies*, vol. 5, no. 2, pp. 1–26, 2021.
- [23] G. Saleem, U. I. Bajwa, and R. H. Raza, “Toward Human Activity Recognition: A Survey,” *Neural Computing and Applications*, vol. 35, no. 5, pp. 4145–4182, 2023.
- [24] N. Bento, J. Rebelo, M. Barandas, A. V. Carreiro, A. Campagner, F. Cabitza, and H. Gamboa, “Comparing Handcrafted Features and Deep Neural Representations for Domain Generalization in Human Activity Recognition,” *Sensors*, vol. 22, no. 19, p. 7324, 2022.
- [25] T. Shen, I. Di Giulio, and M. Howard, “A Probabilistic Model of Human Activity Recognition with Loose Clothing,” *Sensors*, vol. 23, no. 10, p. 4669, 2023.
- [26] R. Hu, L. Chen, S. Miao, and X. Tang, “SWL-Adapt: An Unsupervised Domain Adaptation Model with Sample Weight Learning for Cross-user Wearable Human Activity Recognition,” in *Proceedings of the AAAI Conference on Artificial Intelligence*, vol. 37, no. 5, 2023, pp. 6012–6020.
- [27] W. Lu, J. Wang, X. Sun, Y. Chen, and X. Xie, “Out-of-Distribution Representation Learning for Time Series Classification,” in *Proceedings of the 11th International Conference on Learning Representations (ICLR 2023)*, 2023.
- [28] J. Yang, Y. Xu, H. Cao, H. Zou, and L. Xie, “Deep Learning and Transfer Learning for Device-free Human Activity Recognition: A Survey,” *Journal of Automation and Intelligence*, vol. 1, no. 1, p. 100007, 2022.
- [29] L. Chen, Y. Zhang, Y. Song, A. Van Den Hengel, and L. Liu, “Domain Generalization via Rationale Invariance,” in *Proceedings of the IEEE/CVF International Conference on Computer Vision*, 2023, pp. 1751–1760.
- [30] Y. Kaya and E. K. Topuz, “Human Activity Recognition from Multiple Sensors Data Using Deep CNNs,” *Multimedia Tools and Applications*, vol. 83, no. 4, pp. 10 815–10 838, 2024.
- [31] H. Wu, Z. Mo, J. Tan, S. He, and S.-H. G. Chan, “Efficient Indoor Localization Based on Geomagnetism,” *ACM Transactions on Sensor Networks (TOSN)*, vol. 15, no. 4, 2019.
- [32] J. Tan, H. Wu, K.-H. Chow, and S.-H. G. Chan, “Implicit Multimodal Crowdsourcing for Joint RF and Geomagnetic Fingerprinting,” *IEEE Transactions on Mobile Computing*, vol. 22, no. 2, pp. 935–950, 2021.
- [33] G. Ouyang and K. Abed-Meraim, “A Survey of Magnetic-field-based Indoor Localization,” *Electronics*, vol. 11, no. 6, p. 864, 2022.
- [34] W. Bao, Q. Yu, and Y. Kong, “Evidential Deep Learning for Open Set Action Recognition,” in *Proceedings of the IEEE/CVF International Conference on Computer Vision*, 2021, pp. 13 349–13 358.
- [35] C. Wang, X. Wang, J. Zhang, L. Zhang, X. Bai, X. Ning, J. Zhou, and E. Hancock, “Uncertainty Estimation for Stereo Matching based on Evidential Deep Learning,” *Pattern Recognition*, vol. 124, p. 108498, 2022.
- [36] A. Pandharipande, C.-H. Cheng, J. Dauwels, S. Z. Gurbuz, J. Ibanez-Guzman, G. Li, A. Piazzoni, P. Wang, and A. Santra, “Sensing and Machine Learning for Automotive Perception: A Review,” *IEEE Sensors Journal*, vol. 23, no. 11, pp. 11 097–11 115, 2023.
- [37] Y. Sun, B. Cao, P. Zhu, and Q. Hu, “Drone-based RGB-infrared Cross-modality Vehicle Detection via Uncertainty-aware Learning,” *IEEE Transactions on Circuits and Systems for Video Technology*, vol. 32, no. 10, pp. 6700–6713, 2022.
- [38] Y. Xu, T. Bai, W. Yu, S. Chang, P. M. Atkinson, and P. Ghamisi, “AI Security for Geoscience and Remote Sensing: Challenges and Future Trends,” *IEEE Geoscience and Remote Sensing Magazine*, vol. 11, no. 2, pp. 60–85, 2023.
- [39] B. Schölkopf, F. Locatello, S. Bauer, N. R. Ke, N. Kalchbrenner, A. Goyal, and Y. Bengio, “Toward Causal Representation Learning,” *Proceedings of the IEEE*, vol. 109, no. 5, pp. 612–634, 2021.
- [40] J. Gawlikowski, C. R. N. Tassi, M. Ali, J. Lee, M. Humt, J. Feng, A. Kruspe, R. Triebel, P. Jung, R. Roscher *et al.*, “A Survey of Uncertainty in Deep Neural Networks,” *Artificial Intelligence Review*, vol. 56, no. Suppl 1, pp. 1513–1589, 2023.
- [41] A. Jøsang, *Subjective logic*. Springer, 2016, vol. 3.
- [42] H. Liu, R. Li, S. Liu, S. Tian, and J. Du, “SmartCare: Energy-efficient Long-term Physical Activity Tracking Using Smartphones,” *Tsinghua Science and Technology*, vol. 20, no. 4, pp. 348–363, 2015.
- [43] A. Krizhevsky, I. Sutskever, and G. E. Hinton, “Imagenet Classification with Deep Convolutional Neural Networks,” *Advances in Neural Information Processing Systems*, vol. 25, 2012.
- [44] P. Thiagarajan, P. Khairnar, and S. Ghosh, “Explanation and Use of Uncertainty Quantified by Bayesian Neural Network Classifiers for Breast Histopathology Images,” *IEEE Transactions on Medical Imaging*, vol. 41, no. 4, pp. 815–825, 2021.

- [45] A. Karandikar, N. Cain, D. Tran, B. Lakshminarayanan, J. Shlens, M. C. Mozer, and B. Roelofs, “Soft Calibration Objectives for Neural Networks,” *Advances in Neural Information Processing Systems*, vol. 34, pp. 29 768–29 779, 2021.

Received 20 February 2007; revised 12 March 2009; accepted 5 June 2009